Accepted Manuscript

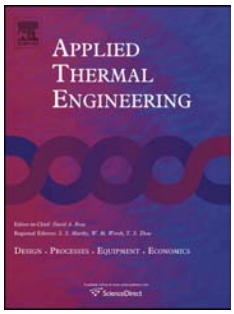

Tuning of thermal properties of sodium acetate trihydrate by blending with polymer and silver nanoparticles

B.M.L. Garay Ramirez, Christ Glorieux, E. San Martin Martinez, J.J.A. Flores Cuautle

PII: S1359-4311(13)00683-2

DOI: 10.1016/j.applthermaleng.2013.09.049

Reference: ATE 5065

To appear in: *Applied Thermal Engineering*

Received Date: 19 June 2013

Revised Date: 23 September 2013

Accepted Date: 25 September 2013

Please cite this article as: B.M.L Garay Ramirez , C. Glorieux, E San Martin Martinez , J.J.A Flores Cuautle , Tuning of thermal properties of sodium acetate trihydrate by blending with polymer and silver nanoparticles, *Applied Thermal Engineering* (2013), doi: 10.1016/j.applthermaleng.2013.09.049.

Tuning of thermal properties of sodium acetate trihydrate by blending with polymer and silver nanoparticles

Garay Ramirez B. M. L.[a], Christ Glorieux[b], San Martin Martinez E.[a]*, Flores Cuautle J. J. A.[b]

[a]Centro de Investigación en Ciencia Aplicada y Tecnología Avanzada del Instituto Politécnico Nacional, Legaria 694. Colonia Irrigación, C.P. 11500, México, D. F., México

[b]Laboratorium voor Akoestiek en Thermische Fysica (ATF), Dep. Physics and Astronomy, Katholieke Universiteit Leuven, Belgium

*To whom correspondence should be addressed.

Dr. Eduardo San Martin Martinez

CICATA-IPN Legaria 694, Col. Irrigacion, C.P. 11500

Mexico, D.F. Mexico, e-mail: esanmartin@ipn.mx

phone/fax: (52) 55-57296300 ext.67769/55-55575103

Highlights

- The addition of silver nanoparticles reduced the supercooling of PCM
- Thermal properties of the PCM are improved with a blend of polymers
- The latent heat recovery of the PCM is higher with silver nanoparticles
- The combination of Polymers and silver nanoparticles reduces the segregation phase.

Abstract

The use of phase change materials (PCMs) is one of the pathways for the storage of temporarily excessive energy from natural sources (solar) and industry for use at a more suitable later time. One of the materials with a high energy storage density is sodium acetate trihydrate (SAT), on which several studies were conducted in order to solve phase segregation and supercooling problems, e.g. by adding polymers and nucleating agents. Here we investigate the effectiveness of adding a polymer blend of carboxymethyl cellulose (CMC) and silica gel to avoid phase segregation, and silver nanoparticles (AgNPs) as nucleating agent. The synthesis of silver nanoparticles was carried out by a green method in CMC as a way to ensure compatibility with SAT. The addition of AgNPs in higher concentrations to 0.5% reduces supercooling, and mixing silica gel with CMC to avoid segregation phase, yields an increment in the stability of the phase change behavior, during heating and cooling cycles. The latent heat release upon crystallization of the PCM was optimum for the mixture with 0.5% AgNPs, and for the highest amounts of CMC with respect to silica gel, with nearly 95% of latent heat recovery compared to pure SAT.

Keywords: carboxymethyl cellulose, silica gel, phase change material, silver nanoparticles, sodium acetate trihydrate, supercooling

Nomenclature

Q	Endothermic heat flow (mW),
To	Onset of melting temperature (ºC),
Tm	melting temperature (ºC),
Tc	crystallization temperature (ºC),
ΔT	Differential temperature between Tm – Tc as supercooling (ºC),
ΔHm	latent heat of fusion (J/g),
ΔHc	latent heat of crystallization (J/g),
PT1000	Platinum resistance thermometers (PRTs)
R^2	determination coefficient,
SD	standard deviation,
P	probability by F test distribution.

Abbreviations

AgNPs, silver nanoparticles; TEM, transmission electron microscopy; RSM, response surface methodology; PCM, phase change materials; SAT, sodium acetate trihydrate; CMC, carboxymethyl cellulose

1. Introduction

There is a clear necessity to rationalize the use of energy in modern society. With this goal several areas of knowledge are exploring options to improve energy efficiency through the development of devices and energy storage systems in order to reduce the mismatch between supply and demand [1]. Energy excess not used in processes should be stored for later use [1, 2]. One of the pathways for storage is the use of phase change materials (PCM), due to their high density of energy storage as latent heat. A great variety of organic and inorganic materials have been studied and selected according to the kind of energy that needs to be stored and transferred to systems or processes [3]. PCMs are nowadays present in

several areas of application, e.g. for building air conditioning [4-6], electronic cooling [7, 8], preservation of food, [9, 10], solar energy storage [11-13], waste heat recovery [14, 15], factories [16] and textiles [17]. The latent heat of PCMs that are based on inorganic salts (250-400 kJ/dm^3) is almost double compared to organic ones (128-200 kJ/dm^3) [18, 19], and they are cheaper and commercially available. However, they have the disadvantage of strong supercooling and they are corrosive in contact with metals [20, 21]. Moreover, under continuous cycles of melting and crystallization, due to the large difference in density between water and the components of the hydrated salt, segregation occurs, resulting in poor crystallization and deteriorating thermophysical behavior. In order to prevent phase segregation it has been proposed to modify the PCM composition to push the material from incongruent to congruent behavior, by adding gelling or thickening materials to avoid segregation, and nucleating agents to reduce supercooling [19, 22].

Since sodium acetate trihydrate (SAT) is an excellent PCM by virtue of its high energy storage density and thermal conductivity, several investigations were conducted to counter the problems above, mainly by using thickening agents such as cellulose derivatives, silica gel, sepiolite, diatomaceous earth [23], starch (wheat flour), methylhydroxyethyl-cellulose, methylcellulose [20], acrylic acid copolymer, carboxymethyl cellulose (CMC), and polyvinyl alcohol (PVA) [24]. Unfortunately gels formed with polymers are highly viscous and difficult to handle. Blending also lowers the energy storage capacity and increases the melting temperature.

In order to reduce supercooling, various (hydrated salt) nucleating agents have been studied, K_2SO_4 [25], $SrSO_4$, $Na_2P_20_7$ $10H_20$ and Carbon (1.5-6.7 µm) [24], NaBr $2H_2O$ or NaHCOO $3H_2O$, polyethylene powder [26], Na_2SO_4 $10H_2O$, Na_2CO_3 $10H_2O$, $Na_4P_2O_7$ $10H_2O$ and Na_3PO_4 $12H_2O$ [27], Na_2HPO_4 $12H_2O$, Na_3PO_4 $12H_2O$, Na_2CO_3 $10H_2O$, Na_2SiO_3 $9H_2O$ and $Na_2B_4O_7$ $10H_2O$ [28]. Overall these nucleation agents decrease the SAT energy storage capacity, and make it less stable, explaining the significant spread in the results.

Also nanoparticles were considered as candidates for serving as nucleating agent by increasing the surface area. Adding 5%wt of Aluminum nitride (AIN) [29], 5%wt or 4%wt Si_3N_4, 10%wt ZrB_2, 2%wt SiO_2, BC_4, SiB_6 has been shown to eliminate the supercooling of SAT [30]. However, the use of high concentrations of nanoparticles is not viable due to the cost of synthesis, problems of homogeneity, and reduction of the heat storage capacity.

In this article we investigate the feasibility of blending small quantities (less than 3%) of (organic) carboxymethyl cellulose (CMC) into SAT to improve its thermal properties, silica gel (inorganic) to limit phase segregation, in combination with Na_2SO_4 and silver nanoparticles (concentration less than 1%) to trigger nucleation and reduce supercooling. The preparation of the samples is described and their characteristics were determined by UV-Vis spectroscopy and Transmission Electron Microscopy (TEM). Their performance as heat storage material was determined by Differential Scanning Calorimetry (DSC) and controlled thermal cycling. Response surface methodology (RSM) is used in order to find the parameters for optimum functionality.

2. Materials and methods

2.1. Materials

For the silver nanoparticle synthesis, silver nitrate ($AgNO_3$, 99.85% Acros Organics), sodium hydroxide (NaOH, 98%), sodium carboxymethyl cellulose (CMC, ≥ 99.5% Sigma-Aldrich), and D-glucose (Bioxtra ≥99.5%, Sigma-Aldrich) were used. The resulting blend was used to improve the characteristics of Sodium Acetate Trihydrate (SAT, Bio ultra, ≥ 99.5% Sigma-Aldrich) provided the heat storage characteristics. Also anhydrous sodium sulfate (ACS reagent, ≥99.0%, Sigma-Aldrich) and silica gel powder (J. T. Baker Chemicals) were blended into the PCM.

2.2. Preparation of silver nanoparticles

Aqueous solutions of CMC (0.54% w/v) and D-glucose (0.25 M) were prepared. After complete dissolution in 90 ml of the water, 10 ml aqueous solution of the Silver Nitrate (0.17 M) was added drop by drop in a three-neck ball glass and further magnetically stirred at 70 ℃. In all experiments deionized water was used (18.2 μΩ/cm), with the pH adjusted to 9.0 by adding NaOH (0.1 N). The solutions turned to a pale orange color after 30s, indicating the initial formation of silver nanoparticles (AgNPs). For all experiments the synthesis was carried out during three hours according to a procedure by Ortega et al [31].

2.3. Characterization of silver nanoparticles

The synthesis of colloidal AgNPs was monitored by acquiring once per hour a UV-Vis spectrum using a 1cm path length quartz cell in Cary 50 spectrometer (Varian, USA), until all changes had ceased. The absorbance of the colloidal solutions was measured in the 300 to 750 nm range. The size and shape of the NPs were determined by transmission electron microscopy (TEM, JEOL-JEM1010 Japan). A drop of the silver AgNPs solution was placed on a carbon-coated copper grid and the average size and distribution of the AgNPs was determined by counting 200 particles in each experiment [32].

2.4. Sample preparation for thermal properties

The blends of SAT, CMC/Silica Gel, AgNPs and Na_2SO_4 were prepared as follows. All samples contained 95% of SAT, 3% of the polymer mixture CMC/silica gel. The remaining 2% consisted of Na_2SO_4 and AgNPs. In view of optimizing the performance of the composite PCM, the following two factors were varied: the fraction of CMC (between 5% and 95%) in the 3% polymer mixture, and the fraction of AgNPs (between 0.08% and 0.92%) within the 2% part of Na_2SO_4 and AgNPs. Response surface methodology was used to design the combinations of these factors to be tested for the corresponding mixtures with respect to (i) the melting temperature, (ii) the crystallization temperature and (iii) their difference, i.e. the degree of supercooling, and also (iv) the melting enthalpy, (v) the crystallization

enthalpy, and (vi) their ratio, i.e. the recovered latent heat fraction. After the AgNPs were synthesized in solution, they were dried out under vacuum at 45 ℃ and then added to the polymer mixture and SAT. The listed amounts of CMC take into account the CMC that was used as passivating agent during AgNPs synthesis, as well as an amount of CMC that was added in the SAT.

2.5. Differential Scanning Calorimetry (DSC)

The thermal properties of the samples were studied by Differential Scanning Calorimetry (DSC) on a Perkin-Elmer Pyris 1 (Perkin Elmer, Norwalk, CT, USA). Indium was used to calibrate the equipment and an empty capsule as reference. The values of the latent heat during melting and crystallization were calculated using Pyris Thermal Analysis Software version 3.01. All samples weights were adjusted to 13.5 ± 2.0 mg and placed in aluminum capsules (No. 0219-0062) that were hermetically sealed. The assays were evaluated in a temperature range from 25 ℃ to 80 ℃, with heating and cooling rates of 5 ℃/min. The degree of supercooling (ΔT) was determined as the difference between the melting (Tm) and crystallization (Tc) temperature.

The fraction of recovered latent heat (%) was determined as:

$$Latent\ heat\ recovered\ (\%) = \frac{\Delta H_c}{\Delta H_m} \times 100$$

with ΔH_m the latent heat of fusion and ΔH_c the latent heat of crystallization

Table 1

2. 6. Stability of SAT-PCM with the polymer blends and silver nanoparticles

The evaluation of heating and cooling cycles was performed in a range from 30 ℃ to 72 ℃. The temperature was measured using a cali brated resistive temperature

detector (RTD PT1000). The temperature records were registered by a homemade LabVIEW 8.5 program (National Instruments). The PT1000 was connected to a multimeter Hewlett Packard 34401A. The sample was heated on a thermal stirrer with temperature control (Cenco Instrumenten, Netherlands).

2.7. Statistical analysis

All experiments were performed in random order and in duplicate. The data were analyzed by response surface methodology (RSM) [33], through Design Expert 8.0 statistical software (State-Ease, Inc.). The experimental design, the independent variables and their variation levels are shown in Table 1. The significance of the mathematical models was tested by using variance analysis (F-test and assessment of the determination coefficient R^2) and the effect of the variables was recorded on response surface graphs [33].

3. Results and Discussion

3.1. UV-Vis spectroscopy of AgNPs

In order to determine the size of the AgNPs, UV-Vis spectra in the range from 300 to 750 nm was acquired. The absorption peak at 420 nm (Fig. 1a) is indicative for the presence of AgNPs, and connected with a surface plasmon resonance [31]. The position of the absorption peak infers a AgNP size between 5 and 10 nm [34]. This was corroborated by transmission electron microscopy (TEM). The absorption spectra of the AgNPs indicate that the distribution of nanoparticles is relatively symmetric and monodisperse with a rather homogeneous size distribution [35].

Fig. 1

After 3 hours of synthesis time the samples were monitored in order to assess the stability of the AgNPs. UV-Vis absorption spectra (Fig. 1b), taken every 24 hours during the first 7 days show a slow increase in absorption. Further increase was confirmed by measurements after 2 and 4 ½ months. Since the peak wavelength did not evolve and the absorption curve remained symmetrical, the increase is probably due to a continuation of nanoparticle formation, and increased the size of

the silver nanoparticles, due to the formation of small clusters or aggregates. Some authors suggest that the growth of the nanoparticles was stabilized after 4 months of storage and depend of the initial concentration of the precursor of Ag^+, the lower concentration of $AgNO_3$ more quickly to stabilize the formation of AgNPs.[34, 35].

3.2. Transmission Electron Microscopy (TEM) of the AgNPs

The nanoparticle size and shape in solution were evaluated after 7 days of formation by means of transmission electron microscopy. Fig. 2a reveals sizes between 3 and 6 nm, with a regular, monodal distribution. Larger sizes were only found in small proportion (Fig. 2b). The shape of the nanoparticles is dominantly spherical [32], and once in a while triangular. The size distribution of AgNPs was found to be monodisperse for these samples. After four months of storage in TEM micrographs of AgNPs was observed larger sizes, this is because initially forming AgNPs cluster and around them are added more AgNPs increasing their size (Fig. not shown). These results are consistent with those observed by the UV-Vis spectra for greater storage time at 4 months.

Fig. 2

3.3. Thermal properties evaluated by differential scanning calorimetry

The DSC thermograms in Fig. 3a illustrate that most of the samples underwent endothermic melting and exothermic crystallization, with characteristics (Table 2) significantly depending on the synthesis. Statistical evaluation by analysis of variances (Table 2) shows that the polynomial models have a significant adjustment to the experimental data by the probability values obtained lower to 1% ($P < 0.01$) and by the coefficients of determination (R^2) greater than 0.87, and the standard deviation values were lower. Except for the crystallization temperature and the degree of supercooling, which have a probability of 0.062 and 0.066 respectively, with a moderated fitting quality ($R^2=0.72$) for both features, the residues do not show deviations from normality, so that the used polynomials models can be used with confidence.

Table 2

Fig. 3a

Fig. 3b

The surface responses in Fig. 3b (a) depict the dependencies of the DSC thermogram features on the synthesis parameters. Upon heating, melting sets on earlier (at lower temperatures) as the AgNPs concentration is higher and the concentration of CMC is lower. It takes less melting energy ΔHm (Fig. 3b (b)) when the concentrations of AgNPs and silica gel are higher. The SAT crystallization temperature (Fig. 3b (c)) is mainly affected by the concentration of AgNPs. A high concentration of AgNPs in combination with a high CMC/silica gel ratio leads to a low crystallization energy ΔHc (Fig. 3b (d)).

A higher concentration (0.8%wt AgNPs) it takes less energy to crystallize the SAT (Fig. 3b(d)), i e that crystallizes at a higher temperature close to its melting temperature, but this behavior is observed only at higher concentrations of CMC (close to 85%). For lower values of the two components the crystallization temperature decreases. The highest concentration of silica (95%) and AgNPs (0.8%) present the lowest crystallization temperature (± 38℃). Probably because the Silica gel polymer favors phase segregation so the SAT not crystallizes at temperatures close to the melting temperature, this behavior is not observed with CMC.

The above results are also reflected in trends in the supercooling of the SAT (Fig. 3b (e)). Less supercooling occurs for high concentrations of AgNPs and CMC (0.85%, 85%). The supercooling of the SAT was remains almost unchanged for lower concentrations of both components CMC and AgNPs.

The highest values of relative recovery of latent heat (with respect to energy needed to melt the substance) are obtained for AgNPs concentrations near 0.4 - 0.6% and concentrations higher than 50% CMC (Fig. 3b (f)). At high concentrations of CMC and AgNPs the recovery of latent heat is low. These results are

corroborated by experimental observations showing that samples that supercool more deeply release more energy upon crystallization.

The stimulation of crystallization by the presence of AgNPs can be explained by the enhanced heterogeneous nucleation. Also their favorable effect on heat transport capacity could play a role in the growth rate of nucleation regions as also observed by [30]. The CMC by chemical structure prevents phase segregation and reduces the energy of crystallization; this behavior was also observed by Hu et al [29]. The silica gel when has a higher concentration facilitate fusion but not the crystallization, nevertheless the two polymers combined promote recovery of latent heat as a function of the AgNPs concentration.

3.4. Stability to heating and cooling cycles

The effect of adding polymers and AgNPs to SAT on the stability during heating and cooling runs is illustrated in Fig. 4, for a low a) (run 10), medium b) (run 2) and high c) (run 4) CMC concentration. The stability was quantified as the number of heating/cooling cycles during which the (shape of the) temperature profile from the liquid to the solid phase was reproducible. For practical reasons, for sample remaining stable for longer than 10 cycles, the number of stable cycles was set to 10.

Fig. 4

The dotted line in the Fig 4 c) represents a measurement carried out one day after the initial one.

With increasing CMC concentration, the blended samples supercool less and show greater stability to repeated cycles of heating and cooling of SAT. The similar behavior between the full and dashed line in run 4 (fig. 4c) confirms that this mixture has a stable thermal cycling behavior. The effect of the CMC concentration on the stability (5 to 95%wt) was statistically evaluated by variance analysis ($P < 0.05$), obtaining the polynomial model shown in Table 2, with a good fit to the experimental data ($R^2 = 0.843$, standard deviation = 1.52). Verification of the

residues has shown that there were no systematic variations between the experimental data and the model, confirming its validity. Moreover, ANOVA analysis has shown that the models (between 6 and 8 fitting parameters) were not overdetermined.

Fig. 5

Fig. 5 shows that by increasing the CMC to silica gel ratio, the number of stable heating/cooling cycles is increasing when the AgNPs concentration was 0.5 to 0.7. By the other side when the concentration of silica gel is increase for the lower AgNPs concentration the continuity of the repeating cycles also is increased. The stability is highest for AgNPs concentrations between 0.7 and 0.5% of the SAT. For higher AgNPs concentration (0.8%) there is a slight decrease in stability, possibly due to the formation of aggregates of AgNPs [30]. The stability is worst for less than 0.2% of AgNPs and for a low CMC concentration in relation of silica gel.

The best conditions for stability (CMC 85%, AgNPs 0.6%) also correspond to the best conditions of latent heat release, indicating that there is a synergy between the factors CMC and AgNPs concentration that favoring latent heat recovery and prevent phase segregation and supercooling.

4. Conclusions

Adding AgNPs to SAT stimulates nucleation and reduces supercooling. The mixture of polymers of CMC and Silica Gel reduce the phase segregation and thus stabilizes SAT through thermal cycling. Especially a large CMC content combined with a large AgNPs concentration goes along with a good stability and latent heat recovery. The silica gel in its highest concentration reduces the energy required for the fusion but not during the crystallization of the SAT.

Acknowledgements

The authors are grateful for the PIFI-SIP IPN and CONACYT sabbatical and postdoctoral scholarships, FWO-Belgium (research project G.0492.10) and KU Leuven (research project OT/11/064) for financial support.

References

[1] Y. Dutil, D.R. Rousse, N.B. Salah, S. Lassue, L. Zalewski, A review on phase-change materials: Mathematical modeling and simulations, Renewable and Sustainable Energy Reviews, 15 (2011) 112-130.

[2] B. Zalba, J.M. Marín, L.F. Cabeza, H. Mehling, Review on thermal energy storage with phase change: materials, heat transfer analysis and applications, Applied Thermal Engineering, 23 (2003) 251-283.

[3] Y. Zheng, W. Zhao, J.C. Sabol, K. Tuzla, S. Neti, A. Oztekin, J.C. Chen, Encapsulated phase change materials for energy storage – Characterization by calorimetry, Solar Energy, 87 (2013) 117-126.

[4] B. Zalba, J.M. Marín, L.F. Cabeza, H. Mehling, Free-cooling of buildings with phase change materials, International Journal of Refrigeration, 27 (2004) 839-849.

[5] A. Pasupathy, R. Velraj, R.V. Seeniraj, Phase change material-based building architecture for thermal management in residential and commercial establishments, Renewable and Sustainable Energy Reviews, 12 (2008) 39-64.

[6] N. Zhu, Z. Ma, S. Wang, Dynamic characteristics and energy performance of buildings using phase change materials: A review, Energy Conversion and Management, 50 (2009) 3169-3181.

[7] F.L. Tan, C.P. Tso, Cooling of mobile electronic devices using phase change materials, Applied Thermal Engineering, 24 (2004) 159-169.

[8] R. Kandasamy, X.-Q. Wang, A.S. Mujumdar, Application of phase change materials in thermal management of electronics, Applied Thermal Engineering, 27 (2007) 2822-2832.

[9] B. Gin, M.M. Farid, The use of PCM panels to improve storage condition of frozen food, Journal of Food Engineering, 100 (2010) 372-376.

[10] E. Oró, L. Miró, M.M. Farid, L.F. Cabeza, Improving thermal performance of freezers using phase change materials, International Journal of Refrigeration, 35 (2012) 984-991.

[11] M.M. Farid, A.M. Khudhair, S.A.K. Razack, S. Al-Hallaj, A review on phase change energy storage: materials and applications, Energy Conversion and Management, 45 (2004) 1597-1615.

[12] A. Shukla, D. Buddhi, R.L. Sawhney, Solar water heaters with phase change material thermal energy storage medium: A review, Renewable and Sustainable Energy Reviews, 13 (2009) 2119-2125.

[13] S.M. Hasnain, Review on sustainable thermal energy storage technologies, Part I: heat storage materials and techniques, Energy Conversion and Management, 39 (1998) 1127-1138.

[14] J. Yagi, T. Akiyama, Storage of thermal energy for effective use of waste heat from industries, Journal of Materials Processing Technology, 48 (1995) 793-804.

[15] T. Nomura, N. Okinaka, T. Akiyama, Waste heat transportation system, using phase change material (PCM) from steelworks to chemical plant, Resources, Conservation and Recycling, 54 (2010) 1000-1006.

[16] N. Sarier, E. Onder, The manufacture of microencapsulated phase change materials suitable for the design of thermally enhanced fabrics, Thermochimica Acta, 452 (2007) 149-160.

[17] S. Mondal, Phase change materials for smart textiles – An overview, Applied Thermal Engineering, 28 (2008) 1536-1550.

[18] S. Himran, A. Suwono, G.A. Mansoori, Characterization of Alkanes and Paraffin Waxes for Application as Phase Change Energy Storage Medium, Energy Sources, 16 (1994) 117-128.

[19] A. Sharma, V.V. Tyagi, C.R. Chen, D. Buddhi, Review on thermal energy storage with phase change materials and applications, Renewable and Sustainable Energy Reviews, 13 (2009) 318-345.

[20] L.F. Cabeza, G. Svensson, S. Hiebler, H. Mehling, Thermal performance of sodium acetate trihydrate thickened with different materials as phase change energy storage material, Applied Thermal Engineering, 23 (2003) 1697-1704.

[21] G.A. Lane, Macro-encapsulation of PCM, in, Vol. Report no. ORO/5117-8, Dow Chemical Company, Midland, Michigan, 1978, pp. 152.

[22] B. Carlsson, H. Stymne, G. Wettermark, An incongruent heat-of-fusion system—CaCl2·6H2O—Made congruent through modification of the chemical composition of the system, Solar Energy, 23 (1979) 343-350.

[23] M Telkes, Solar energy storage, ASHRAE J, 16 (1974) 38.

[24] H.W. Ryu, S.W. Woo, B.C. Shin, S.D. Kim, Prevention of supercooling and stabilization of inorganic salt hydrates as latent heat storage materials, Solar Energy Materials and Solar Cells, 27 (1992) 161-172.

[25] J. Chan Choi, S. Done Kim, G. Young Han, Heat transfer characteristics in low-temperature latent heat storage systems using salt-hydrates at heat recovery stage, Solar Energy Materials and Solar Cells, 40 (1996) 71-87.

[26] H. Kimura, J. Kai, Phase change stability of sodium acetate trihydrate and its mixtures, Solar Energy, 35 (1985) 527-534.

[27] Z.L.L. J. Li, C. F. Ma, , Experimental study on improving solid-liquid phase change performance of acetate hydroxide trihydrate, Journal of Engineering Thermophysics, 27 (2006) 817-819.

[28] J.L. J. Mao, J. Li, G. Peng, J. Li, , A selection and optimization experimental study of additives to thermal energy storage material sodium acetate trihydrate, International Conference on Energy and Environment Technology, (2009) 14-17.

[29] P. Hu, D.-J. Lu, X.-Y. Fan, X. Zhou, Z.-S. Chen, Phase change performance of sodium acetate trihydrate with AlN nanoparticles and CMC, Solar Energy Materials and Solar Cells, 95 (2011) 2645-2649.

[30] Lu. D.-J, Hu. P, Zhao. B.-B, Liu.Y.C, Ze-Shao, Study on the Performance of Nanoparticles as Nucleating Agents for Sodium Acetate Trihydrate, Journal of Engineering Thermophysics, 33 (2012) 1279-1282.

[31] L. Ortega-Arroyo, E.S. Martin-Martinez, M.A. Aguilar-Mendez, A. Cruz-Orea, I. Hernandez-Pérez, C. Glorieux, Green synthesis method of silver nanoparticles

using starch as capping agent applied the methodology of surface response, Starch - Stärke, (2013).

[32] M. Aguilar-Méndez, E. San Martín-Martínez, L. Ortega-Arroyo, G. Cobián-Portillo, E. Sánchez-Espíndola, Synthesis and characterization of silver nanoparticles: effect on phytopathogen Colletotrichum gloesporioides, Journal of Nanoparticle Research, 13 (2011) 2525-2532.

[33] Douglas C. Montgomery, Design and analysis of experiments., John Wiley and Sons, Inc. , New York, 2004.

[34] N. Pradhan, A. Pal, T. Pal, Silver nanoparticle catalyzed reduction of aromatic nitro compounds, Colloids and Surfaces A: Physicochemical and Engineering Aspects, 196 (2002) 247-257.

[35] D.K. Bhui, H. Bar, P. Sarkar, G.P. Sahoo, S.P. De, A. Misra, Synthesis and UV–vis spectroscopic study of silver nanoparticles in aqueous SDS solution, Journal of Molecular Liquids, 145 (2009) 33-37.

Tables Captions

Table 1 Response surface design for SAT, polymer blend and AgNPs

Run	Factor A CMC/GEL (%)	Factor B: AgNPs (%)	Onset (ºC)	Tm (ºC)	ÄHm (J/g)	Tc (ºC)	ÄHc (J/g)	Super cooling (ºC)	Latent Heat (%)
1	50.00	0.92	57.8	62.7	235	59.15	0.1	3.55	0.04
2	50.00	0.50	58.7	63.3	242	51.20	213	12.09	87.95
3	50.00	0.50	59.2	63.3	238	41.32	167	21.95	69.93
4	99.50	0.50	59.1	62.2	234	44.66	208	17.59	88.85
5	15.00	0.80	57.8	63.7	222	38.34	182	25.35	81.81
6	85.00	0.80	58.7	63.9	236	59.21	0.1	4.69	0.04
7	50.00	0.50	59.3	62.8	242	47.78	204	15.06	84.22
8	50.00	0.08	61.3	63.3	251	50.38	209	12.88	83.06
9	15.00	0.20	60.5	62.6	251	49.78	215	12.85	85.87
10	0.50	0.50	58.2	62.5	239	49.43	0.3	13.03	0.12
11	85.00	0.20	59.8	64.5	246	49.24	210	15.21	85.49
12	50.00	0.50	59.5	63.5	237	52.46	207	11.08	87.63
13	50.00	0.50	58.9	65.3	241	49.34	210	15.99	87.33

Table 2 Polynomial regression coefficients of the AgNPs concentration and CMC/gel concentration ratio dependence of the features of the thermograms of PCM-SAT blends.

Coefficient	Onset (ºC)	ÄHm (J/g)	Tc (ºC)	ÄHc (J/g)	Super cooling (ºC)	Latent Heat (%)	Stability
Intercept	62.13	258.80	41.69	371.51	18.52	165.82	21.86
A	$2.02x10^{-2}$	-0.29	0.23	-0.63	-0.17	-1.08	-0.45
B	-11.21	-13.44	54.26	-1451.19	-43.05	-637.03	-69.34
AB	$5.06x10^{-2}$	0.14	-1.63	30.39	1.42	14.54	1.45
A2	$-5.09x10^{-4}$	$3.64x10^{-3}$	NS	$-4.69x10^{-2}$	NS	$-1.18x10^{-2}$	$1.04 x10^{-3}$
B2	6.96	-54.30	-75.11	1502.81	65.78	647.70	58.27
A2B	$7.07x10^{-4}$	$-1.07x10^{-2}$	NS	$3.47x10^{-2}$	NS	NS	NS
AB2	$-8.30x10^{-2}$	1.37	2.13	-38.07	-1.96	-16.48	-1.22
P	0.003	0.003	0.062	0.009	0.066	0.003	0.031
R^2	0.96	0.96	0.72	0.94	0.72	0.93	0.84
SD	0.30	2.27	4.05	34.67	4.15	13.88	1.52

NS = not significative

Figure Captions

Fig. 1 (a) UV-Vis absorption spectrum of AgNPs synthesized in CMC,
(b) Spectral evolution during long term storage of a colloidal solution of AgNPs.

Fig. 2 TEM micrographs and size distribution histograms of synthesized silver nanoparticles, a) Assay realized to 3 h of synthesis and b) Assay realized after 4 month of synthesis.

Fig. 3a DSC thermograms of a selection of PCM-SAT blends

Fig. 3b Response surfaces of features of DSC thermograms of PCM-SAT blends: a) onset of melting, b) ΔH_m of melting, c) crystallization temperature, d) ΔH_c of crystallization, e) degree of supercooling, f) degree of latent heat recovery

Fig. 4 Temperature evolution during heating and cooling cycles of SAT for a low (left, run 10), medium (middle, run 2) and high (right, run 4) concentration of CMC.

Fig. 5 Stability of the SAT to cycles of heating and cooling

Fig. 1

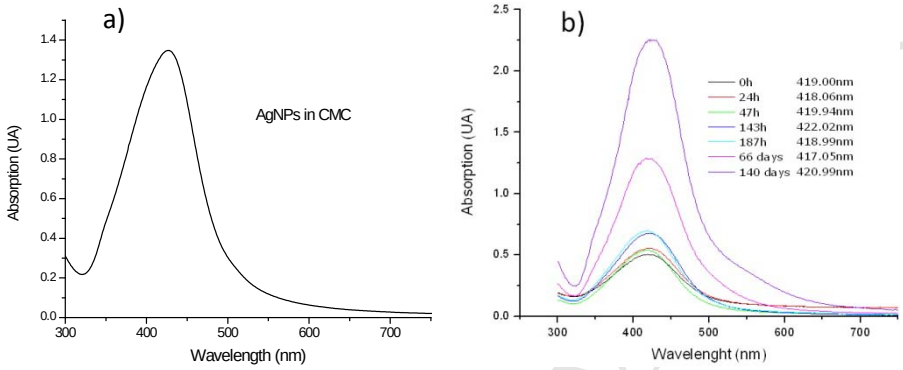

Fig. 2

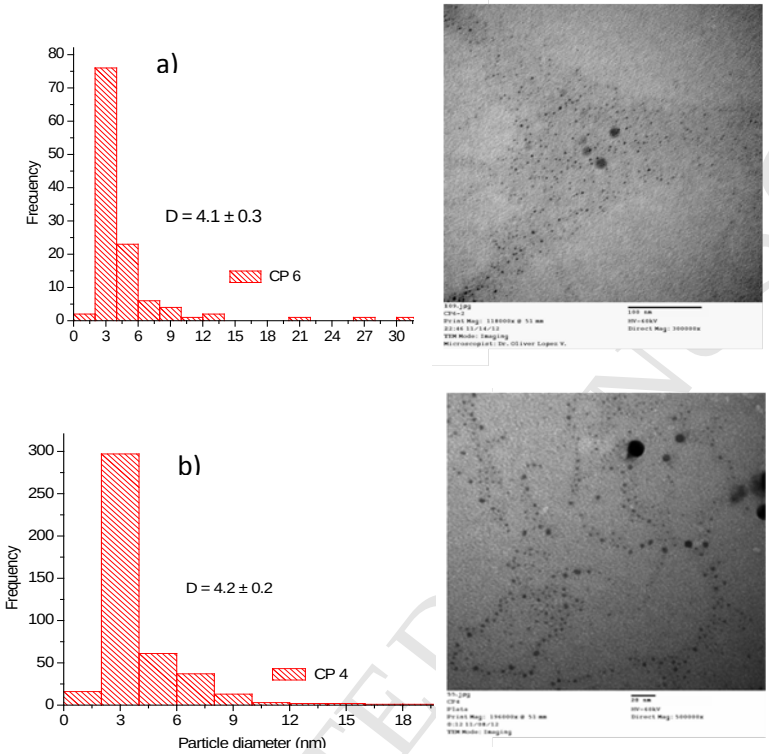

Fig. 3a

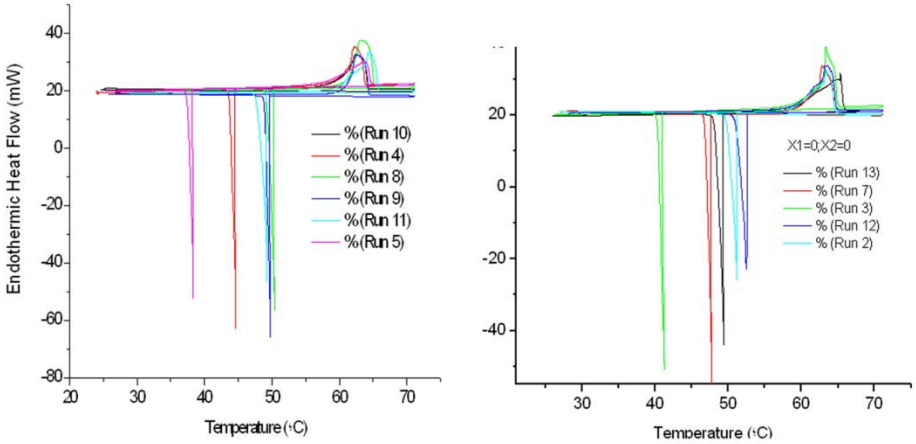

Fig. 3b

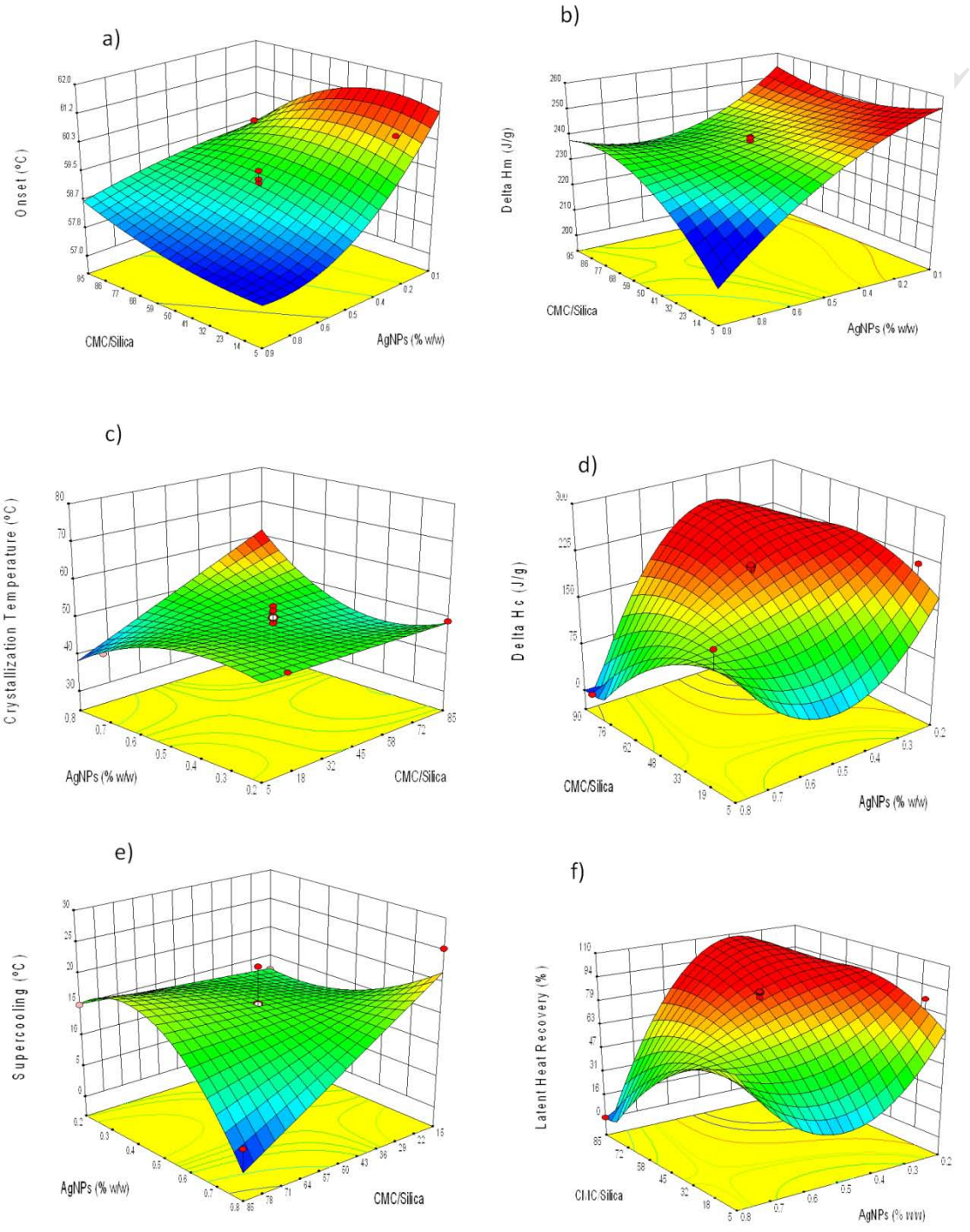
a)
Onset (°C)
CMC/Silica
AgNPs (% w/w)
b)
Delta Hm (J/g)
CMC/Silica
AgNPs (% w/w)
c)
Crystallization Temperature (°C)
AgNPs (% w/w)
CMC/Silica
d)
Delta Hc (J/g)
CMC/Silica
AgNPs (% w/w)
e)
Supercooling (°C)
AgNPs (% w/w)
CMC/Silica
f)
Latent Heat Recovery (%)
CMC/Silica
AgNPs (% w/w)

Fig. 4

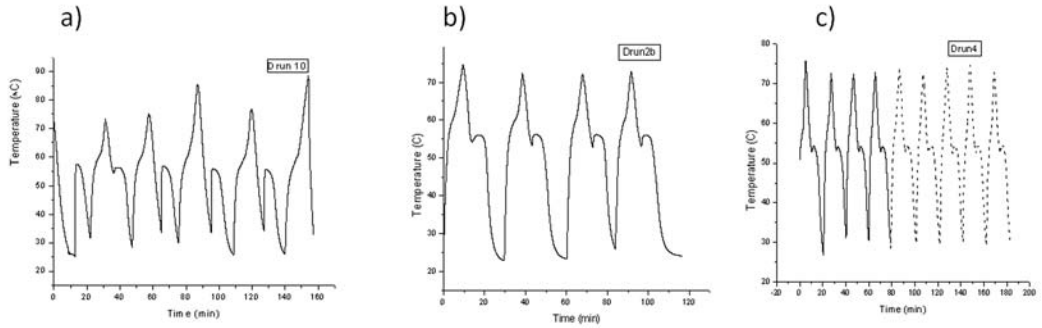

Fig. 5